Control Model for a Solid with a Pore Size Distribution," *AIChE J.*, **19**, p. 259 (1973a).
Hashimoto, K., and P. L. Silveston, "Gasification: Part II. Extension to Diffusion Control," *ibid.*, **19**, p. 268 (1973b).
Hindmarsh, A. C., "Preliminary Documentation of GEARIB: Solution of Implicit Systems of Ordinary Differential Equations with Banded Jacobian," LL Laboratory, UCID-30130 (Feb., 1976).
Howard, J. B., G. C. Williams, and D. H. Fine, "Kinetics of Carbon Monoxide Oxidation in Postflame Gases," 14th Symp. (Int.) on Combustion, p. 975, The Combustion Institute (1973).
Jackson, R., *Transport in Porous Catalysts*, Elsevier, Amsterdam (1977).
Kurylko, L., and R. H. Essenhigh, "Steady and Unsteady Combustion of Carbon," 14th Symp. (Int.) on Combustion, p. 1375, The Combustion Institute (1973).
Laurendeau, N. M., "Heterogeneous Kinetics of Coal Char Gasification and Combustion," *Prog. Energy Comb. Sci.*, **4**, p. 221 (1978).
Madsen, N. K., and R. F. Sincovec, "General Software for Partial Differential Equations," *Numerical Methods for Differential Systems*, L. Lapidus and W. E. Schiesser, Eds., p. 229, Academic Press, New York (1976).
Mon, E., and N. R. Amundson, "Diffusion and Reaction in a Stagnant Boundary Layer about a Carbon Particle. 4: The Dynamical Behavior," *Ind. Eng. Chem. Fund.*, **19**, p. 243 (1980).
Rosner, D. E., and H. D. Allendorf, "Comparative Studies of the Attack of Pyrolytic and Isotopic Graphite by Atomic and Molecular Oxygen at High Temperatures," *A.I.A.A.J.*, **6**, p. 650 (1968).
Ross, I. B., and J. F. Davidson, "The Combustion of Carbon Particles in a Fluidized Bed," *Trans. I. Chem. E.*, **60**, p. 108 (1982).
Simons, G. A., and M. L. Finson, "The Structure of Coal and Char. I. Pore Branching," *Comb. Sci. Technol.*, **19**, p. 217 (1979).
Simons, G. A., "Char Gasification. Part I: Transport Model," *ibid.*, **20**, p. 107 (1979).
Smith, I. W., "The Intrinsic Reactivity of Carbons to Oxygen," *Fuel*, **57**, p. 409 (1978).
Sotirchos, S. V., "Diffusion and Reaction in a Char Particle and in the Surrounding Gas Phase," Ph.D. Dissertation, University of Houston, Houston (1982).
Sotirchos, S. V., and N. R. Amundson, "Diffusion and Reaction in a Char Particle and in the Surrounding Gas Phase. Two Limiting Models," *Ind. Eng. Chem. Fund.* **23**, 180 (1984a).
Sotirchos, S. V., and N. R. Amundson, "Diffusion and Reaction in a Char Particle and in the Surrounding Gas Phase. A Continuous Model," *Ind. Eng. Chem. Fund.* **23**, 191 (1984b).
Sotirchos, S. V., E. Mon, and N. R. Amundson, "Combustion of Coke Deposits in a Catalyst Pellet," *Chem. Eng. Sci.*, **38**, p. 55 (1983).
Srinivas, B., and N. R. Amundson, "Intraparticle Effects in Char Combustion. III. Transient Studies," *Ind. Eng. Chem. Fund.*, **60**, p. 728 *Ind. J., Chem. Eng.*, **59**, 728 (1981).
Sundaresan, S., and N. R. Amundson, "Diffusion and Reaction in a Stagnant Boundary Layer about a Carbon Particle. 7. Transient Behavior and Effect of Water Vapor," *AIChE J.*, **27**, p. 679 (1981).
Ubhayakr, S. K., and F. A. Williams, "Burning and Extinction of a Laser-Ignited Carbon Particle in Quiescent Mixtures of Oxygen and Nitrogen," *J. Electrochem. Soc.*, **123**, p. 747 (1976).
Zamoluev, V. K., L. N. Mukhanova, and E. M. Tait, "The Thermophysical and Mechanical Properties of Highly Carbonized Polymeric Materials," *Proc. Acad. Sci.*, USSR, Chem. Techn. Sect., **133**(5), p. 127 (1960).
Zygourakis, K., L. Arri, and N. R. Amundson, "Studies on the Gasification of a Single Char Particle," *Ind. Eng. Chem. Fund.*, **21**, p. 1 (1982).

Manuscript received January 10, 1983; revision received June 28, 1983 and accepted July 1, 1983.

Part II: Transient Analysis of a Shrinking Particle

The diffusion and reaction model developed in a previous paper is extended allowing for shrinkage of the char particles. It is shown that possible shrinkage, arising from disintegration of the solid structure at a certain conversion level, modifies severely the extinction behavior of the reacting particles. Specifically, the region of ambient temperature and particle radius in which the predictions of the nonisothermal and of the isothermal versions of the model differ significantly becomes smaller. However, the particle shrinkage does not affect the ignition phenomena observed since a particle usually ignites at low conversion levels where the radius change is still negligible.

S. V. SOTIRCHOS and N. R. AMUNDSON

Department of Chemical Engineering
University of Houston
Houston, TX 77004

SCOPE

In Part I, we investigated the transient behavior of char particles in an oxidizing environment. The dynamic model was built on the assumption that the radius of the reacting particles remains constant during the process. This assumption stems from the supposition that the porous solid structure does not collapse at high conversion levels. Several experimental studies, however, indicate that the above may not be true for some types of char. For instance, the char samples used in the experiments of Dutta et al. (1977) disintegrated into smaller fractions at high conversions (above 80%). Also, shrinkage of burning carbon particles in a fluidized-bed combustor is suggested by the experimental data of Ross and Davidson (1982) that show diminishing concentration of CO_2 in the products at intermediate and high conversion levels.

This part of our study focuses on the transient behavior of shrinking particles. As our pseudosteady-state computations (Sotirchos and Amundson, 1984a, b) and the results in Part I have shown, the solution structure of the system depends strongly on the size of the particle and on the intraparticle thermal gradients. Because of the very low thermal conductivity of the ash layer and of the high conversion layers that surround the inner core of a reacting particle, possible particle shrinkage has a direct effect not only on the size of the particle but also on the intraparticle temperature differences. Consequently, significant differences between the behavior of shrinking and nonshrinking particles must be expected.

To allow for changes in the particle size, we assume that shrinkage arises from disintegration of the solid structure at some conversion level which is treated as a model parameter. Our analysis chiefly concentrates on the changes introduced in the extinction behavior of the reacting particles. As the results from the transient model for particles of constant radius (See Part 1) have shown, the particles usually ignite at low average conversion levels, where the conversion at the surface of the particle is well below the disintegration threshold.

Present address of S. V. Sotirchos: Department of Chemical Engineering, University of Rochester, Rochester, NY 14627.

CONCLUSIONS AND SIGNIFICANCE

The extinction behavior of burning char particles is severely modified when disintegration of the solid structure at a certain conversion level is introduced in the transient model. Shrinking, nonisothermal char particles suffer extinction at lower conversion levels than the respective nonshrinking particles, but the opposite phenomenon is observed for isothermal particles. This behavior leads to considerably smaller differences between the quantitative predictions of the isothermal and of the nonisothermal versions of the dynamic model, and it narrows the region of ambient temperature and particle radius in which the results of the two versions differ significantly.

Initially, a shrinking particle burns like a nonshrinking one, i.e., at constant radius and decreasing density. When the conversion at the surface of the particle reaches the critical value, the particle starts to shrink and practically burns at constant density as long as it is on the ignited branch of the solution and away from the lower bound of the multiplicity region. The average density decreases noticeably in the vicinity of the average conversion value at which the particle suffers extinction and in the kinetically controlled regime. Similar behavior of radius and density over a wide range of average conversion has been exhibited by an isothermal film model developed by Gavalas (1981). As the particle temperature remains constant during the process, however, the concepts of ignition and extinction do not apply to the above model.

As in the case of the constant radius model, unlike modes of pore structure evolution lead to extinction at different conversion levels. In general, the effect of the pattern of pore structure evolution on the extinction phenomena observed is very strong, especially in the vicinity of the initial multiplicity region. Consequently, the shrinking core model, which is independent of the internal pore structure, appears to be inadequate for transient computations in a wide range of ambient temperature and particle size.

DEVELOPMENT OF THE MODEL COMPUTATIONAL ASPECTS

The mass and energy balance equations, the flux relations, the carbon mass balance in the interior of the particle, as well as the associated boundary and initial conditions are identical to those relations used in the development of the constant radius model in Part I. The above is also true for the dimensionless form of the equations (Eqs. 12–17 in Part I) where the dimensionless variables and constants are now based on the initial radius of the particle, a_o. Thus, the conditions at $\zeta = 1$ and $\zeta = \beta$ are respectively set at $\zeta = \alpha$ and $\zeta = \beta'$ where

$$\alpha = \frac{a}{a_o} \quad \text{and} \quad \beta' = \frac{b}{a_o} . \tag{1}$$

Obviously, α and β' are functions of time. The relation between a and b—and consequently between α and β'—can be found in general using correlations of the Nusselt or Sherwood numbers found in the literature. However, in accordance with our previous assumptions, we will again assume that the thickness of the boundary layer remains equal to one particle radius.

The moving boundaries can be immobilized by introducing two new independent variables, ζ' and τ', which in terms of the old independent variables are given by the relations

$$\tau' = \tau \quad \text{and} \quad \zeta' = \frac{\zeta}{\alpha} . \tag{2}$$

Applying the chain rule of differentiation, it can be shown that the partial derivatives of any dependent variable must satisfy the relations

$$\left(\frac{\partial}{\partial \zeta}\right) = \frac{1}{\alpha}\left(\frac{\partial}{\partial \zeta'}\right) \tag{3a}$$

$$\left(\frac{\partial}{\partial \tau}\right) = \left(\frac{\partial}{\partial \tau'}\right) - \frac{\zeta'}{\alpha}\left(\frac{\partial}{\partial \zeta'}\right)\left(\frac{d\alpha}{d\tau'}\right) \tag{3b}$$

where $d\alpha/d\tau'$ is the shrinkage rate of the particle. Equations 3 can be used to transform the dimensionless differential equations and the boundary conditions at $\zeta = 0$, $\zeta = \alpha$, and $\zeta = \beta'$ for the moving boundary problem (Eqs. 12–16 in Part I) to the respective differential equations and boundary conditions at $\zeta' = 0$, $\zeta' = 1$, and $\zeta' = \beta$ for the immobilized boundary problem. The initial conditions of the new problem are still given by Eq. 17 in Part I. If the particles behave isothermally, the energy condition at the surface is substituted by an overall energy balance, similar to Eq. 18 in Part I, derived by integrating the energy equation in the interior of the particle and using the energy boundary condition at the surface.

Solution of the transformed energy and mass balance equations requires knowledge of the shrinkage rate of the particles. Our pseudosteady state computations (Sotirchos and Amundson, 1984a, b) have shown insignificant contribution of the occurrence of the heterogeneous reactions on the external surface of the particle to the overall combustion rate, even at high temperatures. Therefore, reaction on the external surface of the particle alone would not produce any significant change in the radius of the particle within the particle lifetime. Several investigators postulated other mechanisms in order to explain the higher shrinkage rates. In a gasification study of single char particles, Hashimoto and Silveston (1973a, b) considered that shrinkage arises from gasification of the material on the external surface of the particle and from abrasion of the particle. The latter was assumed to be a constant fraction of the gasification rate on the external surface area. In another gasification study, Groeneveld and van Swaaij (1980) considered that the particle shrinks because of disintegration of the solid structure at a critical conversion level. This assumption was also used by Gavalas (1981) when he investigated the combustion of single char particles by use of an isothermal film model employing the pore structure evolution model he had presented previously (Gavalas, 1980). The disintegration assumption is partially supported by the experimental observations of Dutta et al. (1977) who noticed that at high conversion levels the reacting char particles broke into smaller fractions.

In this study, we consider that disintegration of the solid structure at a certain conversion level, ξ^*, is the sole cause of particle shrinkage. Therefore, the radius of the particle remains constant as long as the conversion at its surface is lower than ξ^*. When the conversion at the surface reaches the disintegration value, the structure starts to collapse locally, and the boundary recedes keeping the conversion at the surface equal to ξ^*. As Gavalas (1981) pointed out, this is equivalent to setting

$$\left(\frac{\partial \xi}{\partial \tau'}\right) = 0 \qquad \text{at } \zeta' = 1 \qquad \text{if } \xi = \xi^* . \tag{4}$$

Introducing Eq. 4 in Eq. 3b and rearranging, one obtains the following equation for the shrinkage rate of the particle (Gavalas, 1981):

$$\frac{d\alpha}{d\tau'} = \begin{cases} 0 & \text{if } \xi(1,\tau') < \xi^* \\ -\alpha\left(\dfrac{\partial \xi}{\partial \tau}\right)\Big|_{\zeta=\alpha} \Big/ \left(\dfrac{\partial \xi}{\partial \zeta'}\right)\Big|_{\zeta'=1} & \text{if } \xi(1,\tau') = \xi^*, \end{cases} \tag{5a}$$

with

$$\alpha = 1 \qquad \text{at } \tau' = \tau = 0. \tag{5b}$$

Thus, the combustion problem of a shrinking char particle is described by the transformed energy and mass balance equations developed in Part I (Eqs. 12–17) and by Eq. 5.

The above problem is solved employing the numerical method used for the constant radius model, described extensively in Part I. More details for this particular application are given by Sotirchos (1982).

RESULTS AND DISCUSSION

As in Part I, we present results for spherical IGT Char #HT155 particles reacting in air at atmospheric pressure with 0.5% water vapor present. We use the single particle radiation scheme and the same values for the parameters of the model as in Part I and assume that the stagnant film thickness is equal to one particle radius. The initial conditions used refer to particles of uniform temperature in an inert atmosphere introduced into the reactive environment at time zero. It must be pointed out, however, that the results are practically insensitive to changes in the initial values of the concentrations since the concentration profiles adjust themselves to the boundary conditions before any significant change in the particle temperature and in the conversion takes place.

It must have become obvious from the development of the model that unless the slope of the conversion profile at the external surface of the particle is positive, at least when the surface conversion attains values close to the critical value, Eq. 5 is physically meaningless—since it then predicts increase of the radius of the particle with time. When the conversion reaches the critical value earlier at some point in the interior of the particle than at the surface, the solid structure also collapses earlier at this point, and consequently our analysis is not applicable. As the results from the constant radius model have shown (Part I) this situation is quite common for nonisothermal P1 particles reacting in the kinetically controlled or in the transition regime of the initial pseudosteady state locus. The above observation does not apply to isothermal particles for the conversion always increases monotonically with the distance.

Shrinking Core Pseudosteady-State Structure

Before we investigate the transient behavior of the system, it will be useful to examine how disintegration of the ash layer influences the pseudosteady state structure of a particle burning in a shrinking core fashion. The situation results when both oxygen and carbon dioxide are depleted as soon as they reach the external edge of the unreacted core and consequently it is not very common for the real problem. The C-CO_2 reaction becomes diffusionally controlled only at very high temperatures, and in the most interesting region of intermediate temperatures the penetration depth of oxygen into the "unreacted" core is not zero. However, when the particle reacts in an ignited state, conversion changes mostly occur in a thin shell close to the surface of the particle. Therefore, the analysis of the shrinking core pseudosteady state structure may provide useful pieces of information regarding the effects of possible particle shrinkage on the extinction characteristics of the process. It is important to observe that construction of the shrinking core PSS structure does not require solution of the transient model.

Figure 1 presents the pseudosteady-state locus of a nonisothermal particle (0.2 mm) at several levels of average conversion for shrinking core behavior. When the radius of the particle remains constant (Figure 1a), the ignition limit (upper bound of the multiplicity region) increases, while the multiplicity region itself becomes larger. Its lower bound moves towards lower temperatures, and the upper ignited branch of the solution exists in a wider temperature region. At about 50% conversion, the PSS locus of a constant radius particle starts to shift to the right, but even at 90% conversion the ignited branch of the solution vanishes only from a small part of the regime in which it was initially present. Thus, most particles that start burning at $t = 0$ along the ignited branch of the solution will probably be in an ignited state even beyond 90%

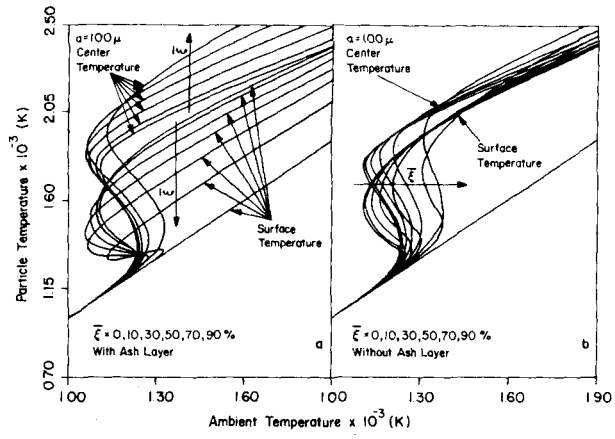

Figure 1. Comparison of the pseudosteady-state loci of a nonisothermal particle with and without ash layer around it at several levels of average conversion for shrinking core behavior.

conversion. Indeed, as the transient computations in Part I have shown, this is true. Another observation from Figure 1a, which also agrees with the results of the constant radius model, is that the temperature difference between center and surface rises rapidly with increasing conversion.

The behavior of the pseudosteady state locus is completely different if the ash layer left after depletion of the combustible material peels off. As Figure 1b shows, reducing the particle size the PSS locus unfolds progressively to the right, the ignition ambient temperature increases, and the multiplicity region shrinks. For instance, nonisothermal shrinking particles with 0.2 mm initial diameter that react along the ignited branch of the PSS structure in the region 1,110–1,350 K may suffer extinction at some conversion level lower than 90%.

This different behavior is principally caused by the very low thermal conductivity of the ash layer that surrounds the unreacted core of a nonshrinking particle, which leads to large temperature differences between the unreacted core and the surface of the particle. Since the particle reacts at high temperature (the average temperature of the inner core) and loses heat at progressively lower surface temperature, an ignited state can be sustained even at high conversion levels. On the other hand, there are no major changes in the magnitude of the intraparticle temperature differences of a shrinking particle. However, the external surface area to volume ratio takes on higher values, and the particle loses relatively larger amounts of heat by radiation and conduction. As a result, the ambient ignition temperature increases, and the pseudosteady-state solution locus moves towards higher temperatures. The combustion rate of a nonshrinking particle is considerably lower at high conversion levels, because the reactants must also diffuse through the ash layer in order to reach the unreacted core. The strong effect of the lower surface temperatures, however, on the radiant interaction of the particle with the environment counterbalances the effects of the lower reaction rates.

The pseudosteady-state results for an isothermal particle, on the other hand, show that the ignited branch of the PSS locus of a nonshrinking particle vanishes at lower conversions. Figure 2b is qualitatively similar to Figure 1b, but the behavior exhibited by the PSS locus of a nonshrinking, isothermal particle (Figure 2a) is completely different from what Figure 1a presents. The T_p vs. T_b locus in Figure 2a unfolds so rapidly to the right with increasing conversion that at about 40% average conversion $T_b(T_p)$ is a monotonically increasing function. On the contrary, the shrinking particle model predicts multiple solutions even at 90% conversion.

Therefore in the actual problem of shrinking particles, the large differences between the burning times of isothermal and nonisothermal particles caused by the earlier extinction of the former (Part I) may be confined in a considerably narrower region of

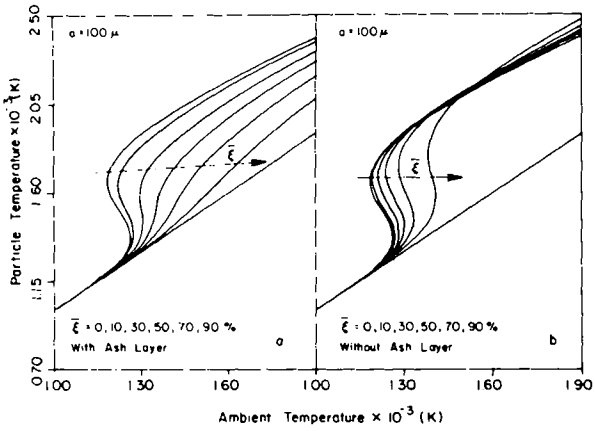

Figure 2. Comparison of the pseudosteady state loci of an isothermal particle with and without ash layer around it at several levels of average conversion for shrinking core behavior.

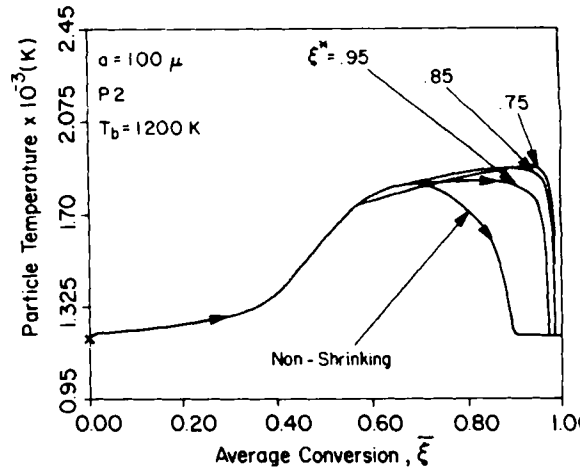

Figure 4. Temperature histories of an isothermal P2 particle for several values of critical conversion with T_o = 1,200 K.

temperature and radius. Disintegration of the ash layer influences differently the behavior of isothermal particles because the results are independent of the actual thermal conductivity of the intraparticle region. At some conversion level, the shrinking particles exhibit higher combustion rates and radiate heat through a smaller surface area. As a result, the ambient temperature corresponding to a certain particle temperature must be lower for a shrinking particle so that the larger amount of heat released in the system can be transferred to the environment.

As we pointed out before, a char particle burns in a shrinking core fashion only at unreasonably high temperatures. Usually, reaction occurs in a shell of finite thickness surrounding the "unreacted" core of the particle. The partially reacted solid is characterized by low thermal conductivity which can lead to considerably higher temperature differences in the intraparticle region. Also, depending on the pattern of pore structure evolution (Figure 1 in Part I), the partially reacted layers of solid may be less or more reactive than the unreacted material. For both reasons, although the shrinking core PSS structure depends only on the initial pore structure properties of the char sample, transient computations may also reveal differences among shrinking particles characterized by dissimilar modes of pore structure evolution. For a char of given properties, however, the actual transient behavior of ignited shrinking particles must agree qualitatively with the predictions of the shrinking core PSS structure.

Results from the Transient Analysis of the System

Figures 3 and 4 present temperature histories of shrinking char particles in terms of the variation of the surface and center temperature of the particle or of the isothermal particle temperature with the conversion. Several values of critical conversion level have been used, and the transient paths followed by the respective nonshrinking particles are also shown in the figures. The average conversion used is based on the combustible material left on the reacting particle; that is, it also includes the carbon lost in the ash. At the point where a particle starts to shrink, its shrinkage rate is discontinuous, jumping from zero to a finite value. For this reason, the slopes of the curves T_s, T_c vs. $\bar{\xi}$ or T_p vs. $\bar{\xi}$ also go through a sharp change at this point (Figures 3-6). Before we discuss the transient results, we need point out that at temperatures lying in the lower part of the multiplicity region, our shrinking particle analysis might not be applicable to non-isothermal particles. In this temperature range, the conversion profile presents a maximum in the interior of the particle (see Figure 18 in Part I), and consequently disintegration of the solid structure may not start first at the external surface of the particle. This phenomenon is more pronounced for nonisothermal particles with low initial temperature and high critical conversion level.

In general, the dynamic behavior of the reacting particles agrees qualitatively with the shrinking core PSS structure. As Figure 3 shows, ignited non-isothermal particles suffer extinction at lower conversion levels if they shrink in the course of their combustion. On the contrary, decreasing the critical conversion level, ignited isothermal particles fall to the unignited branch at progressively higher conversion. The sensitivity of the results to $\bar{\xi}^*$ decreases drastically as its value rises. For instance, in Figure 4 the temperature histories for 75 and 85% critical conversion lie close to each

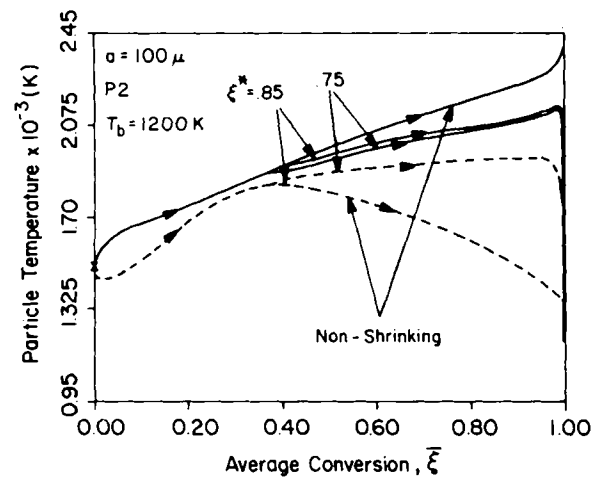

Figure 3. Temperature histories of a nonisothermal P2 particle for several values of critical conversion with T_o = 1,500 K. ——: center-temperature, - - - -: surface temperature.

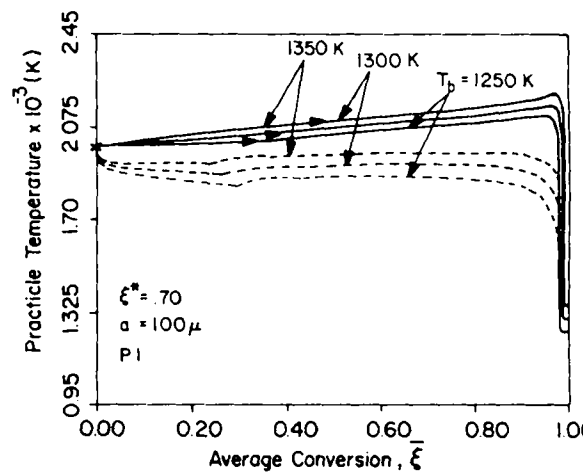

Figure 5. Temperature histories of a shrinking, nonisothermal P1 particle at several ambient temperatures with T_o = 2,000 K. See Figure 3.

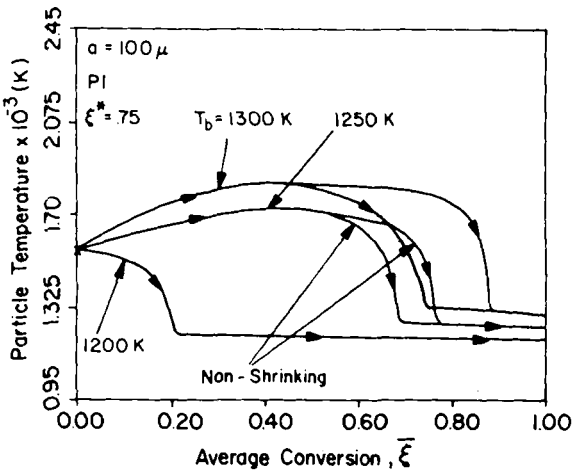

Figure 6. Temperature histories of a shrinking, isothermal $P1$ particle at several ambient temperatures with T_o = 1,550 K.

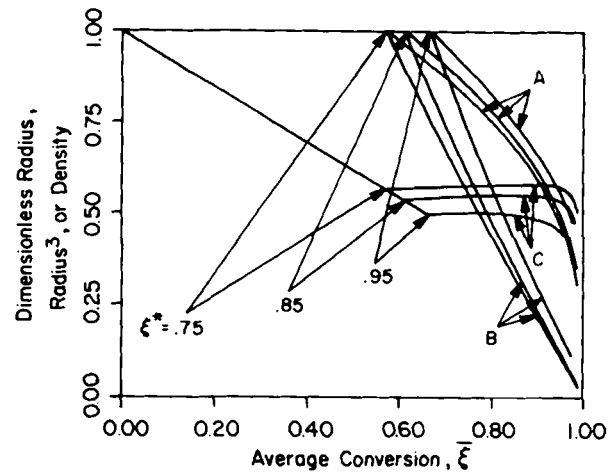

Figure 8. Variation of radius and density with the average conversion for the particles of Figure 4. See Figure 7.

other and away from the transient path of 95% critical conversion.

The inner core of the ignited char particles is surrounded by a partially converted layer of finite thickness that causes their transient behavior to deviate quantitatively from the predictions of the shrinking core PSS structure. In general, the presence of these partially reacted layers around the "unreacted" core shifts the actual pseudosteady state locus towards lower temperatures. This trend is more pronounced for $P2$ particles because the partially converted material may be more reactive than the inner core (Figure 1 in Part I). As a result, the upper ignited branch of the solution vanishes at higher conversion levels, and the ignited particles suffer extinction at considerably higher conversions. For example, the shrinking particles of Figure 3 fall to the unignited branch at 99% conversion although the shrinking core results of Figure 1 predict extinction at about 70% conversion. Moreover, one must take into account the thermal inertia of the reacting particles. Though extinction takes place in a fraction of the total burning time, significant changes of conversion may take place during this time interval.

The effect of particle shrinkage on the extinction behavior of non-isothermal particles may be seen more clearly in Figure 5. At the same conditions, the respective non-shrinking particles are quenched beyond 99% convesion, as Figure 19 in Part I implies. Figure 5 also presents the effect of ambient temperature on the conversion value at which extinction occurs. Increasing the ambient temperature, the particle falls to the unignited branch with higher average conversion, and it starts to shrink at lower conversion levels.

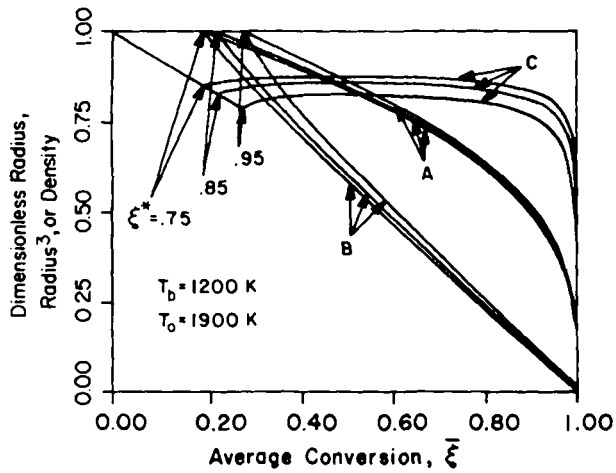

Figure 7. Variation of radius and density with the average conversion for a 200 μ nonisothermal $P2$ particle. A: variation of radius, B: variation of cube of radius, C: variation of density.

Also, the center and surface temperatures take on higher values, but their difference decreases indicating that the particle approaches more closely the shrinking core behavior.

The ambient temperature influences similarly the behavior of isothermal $P1$ particles (Figure 6). The particles of Figure 6 suffer extinction at higher conversions than the respective nonshrinking particles but with considerably lower average conversion than $P2$ particles reacting at the same conditions. For instance, the $P1$ particle of Figure 6 reacting at 1,300 K falls to the unignited branch with lower average conversion than the $P2$ particle of Figure 4 that reacts at 1,200 K. The behavior of isothermal $P1$ particles, however, agrees quantitatively with the shrinking core PSS structure. The conversion at the external surface of the particle reacting at 1,200 K does not reach the disintegration threshold before the particle suffers extinction. For this reason, both shrinking and nonshrinking particles follow the same transient path up to high conversion values.

The variation of the radius of the particle with the average conversion offers another interesting and very informative representation of the transient paths followed by the shrinking particles (Figures 7–10, curves A and B). Instead of the particle radius, one can equivalently use the average density of the particle which relates to the particle radius through the equation

$$\bar{\xi} = (1 - \rho_p/\rho_{po})\alpha^3/W_b + (1 - \alpha^3). \qquad (6)$$

Initially, the radius of the particle remains constant, and the average density, according to Eq. 6, is proportional to $(1 - \bar{\xi})$. When the particles start to shrink, their average density remains almost constant in a wide range of average conversion and experiences only a minor increase (Figures 7, 8 and 9) or decrease (Figure 10)

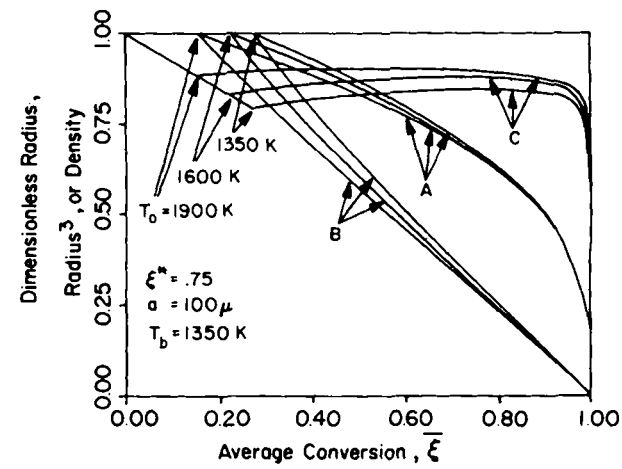

Figure 9. Variation of radius and density of a shrinking, nonisothermal $P2$ particle with the conversion and the initial temperature. See Figure 7.

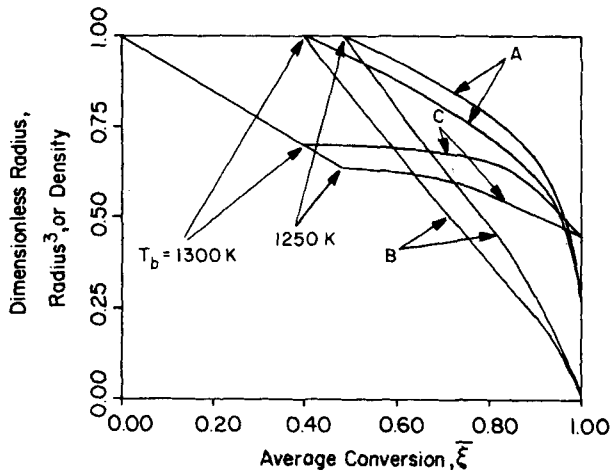

Figure 10. Variation of radius and density with the conversion for the particles of Figure 6. See Figure 7.

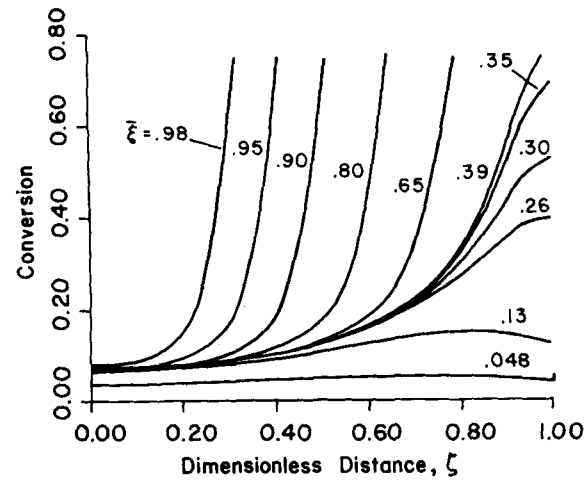

Figure 11. Conversion profiles of the shrinking, nonisothermal P2 particle of Fig. 3 with 75% critical conversion.

depending on how the conversion profile evolves with the average conversion. In the same average temperature range, there is an almost linear relation between the cube of the radius of the particle and the average conversion, as expected from Eq. 6. At conversion levels close to the value where a reacting particle suffers extinction, conversion changes take place throughout the particle, and the density starts to decrease noticeably. For shrinking core behavior, the density of the particle remains constant while the cube of its radius varies proportionally to $(1 - \bar{\xi})$. Indeed, decreasing the critical conversion level (Figures 7 and 8), increasing the ambient temperature (Figure 10), and increasing the initial temperature (Figure 9), paths B and C move closer to the limiting curves for shrinking core behavior. Again, notice that at the point where the particles start to shrink all curves go through a sharp slope change owing to the discontinuity of the shrinkage rate of the particle, Eq. 5a.

Figure 10 shows clearly how the average density and particle radius vary with the average conversion after an ignited particle suffers extinction. For instance, the isothermal particle reacting at 1,300 K is quenched at about 88% conversion (Figure 6). Since in the kinetically controlled regime reaction occurs throughout the particle, the rate of change of the cube of the radius with the conversion decreases. At the limit of complete conversion, the radius approaches zero, and the average density takes on the value that corresponds to the critical conversion level, $(1 - \xi^* W_b)$.

Figure 11 gives the evolution of the conversion profile of a nonisothermal particle whose temperature history is shown in Figure 3. Initially the particle moves towards the ignited branch of the solution, its temperature is not very high, and considerable conversion changes occur throughout its volume. When disintegration starts, the boundary recedes keeping the conversion at the surface constant, and combustion occurs only in a thin region close to the external surface of the particle. Similar is the behavior of the conversion profile of an isothermal particle shown in Figure 12. As the isothermal particle approaches the conversion value where it suffers extinction (Figure 6), noticeable conversion changes take place at its center, and its density starts to decrease (Figure 10). The slope of the conversion profile at the external surface of a nonisothermal particle increases as the particle starts to shrink (Figure 11), and consequently the shrinkage rate of the particle decreases (Eq. 5a). This phenomenon compares with the negative slope of the conversion profile at the external surface of nonisothermal particles that react at ambient temperatures lying close to the lower bound of the initial multiplicity region (Figure 18 in Part I). Hence, it is more pronounced for high critical conversions (Figure 7), for low initial temperatures (Figure 9), and a low ambient temperatures (compare Figures 7 and 9). The conversion profile of an isothermal particle, however, does not change markedly close to the external surface after disintegration of the particle starts (Figure 12), and less significant changes of average density are observed (Figures 8 and 10).

Some results for the relative amount of CO leaving the edge of the stagnant film as CO_2 are shown in Figure 13. As the pseudo-steady state analysis of the problem has also shown, the amount of CO_2 produced decreases strongly with decreasing ambient temperature or particle size. At the conditions of Figure 13, the reacting particles are well inside the ignition regime of the initial PSS locus (Figure 2 in Part I), and consequently they move towards the ignited branch of the solution very fast. As a result, combustion occurs in a thin shell close to the external surface and the surface of the particle is at considerably higher temperature than its center. The surface temperature of the particles goes through a maximum, and since the oxidation of CO takes place close to the external surface of the particle, the CO_2/CO ratio presents a maximum too. When the nonshrinking particles start to react along the ignited branch of the solution, however, the CO_2/CO ratio starts to rise again, because the produced CO must travel a much longer distance in order to reach the outer edge of the stagnant film.

The behavior exhibited by nonshrinking particles is at variance with some results from fluidized bed combustion experiments (Ross and Davidson, 1982) that show decreasing concentration of CO_2 in the products at intermediate and high conversions. The shrinking particle results (solid curves), however, agree qualitatively with the above experimental data. At the point where disintegration of the porous structure and, hence, shrinkage of the particles start, the shrinking particle results depart from the nonshrinking particle

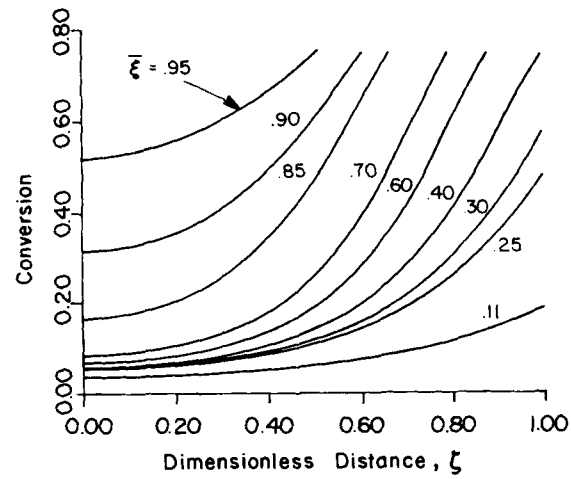

Figure 12. Conversion profiles of the shrinking, isothermal P1 particle of Figure 6 at 1,300 K.

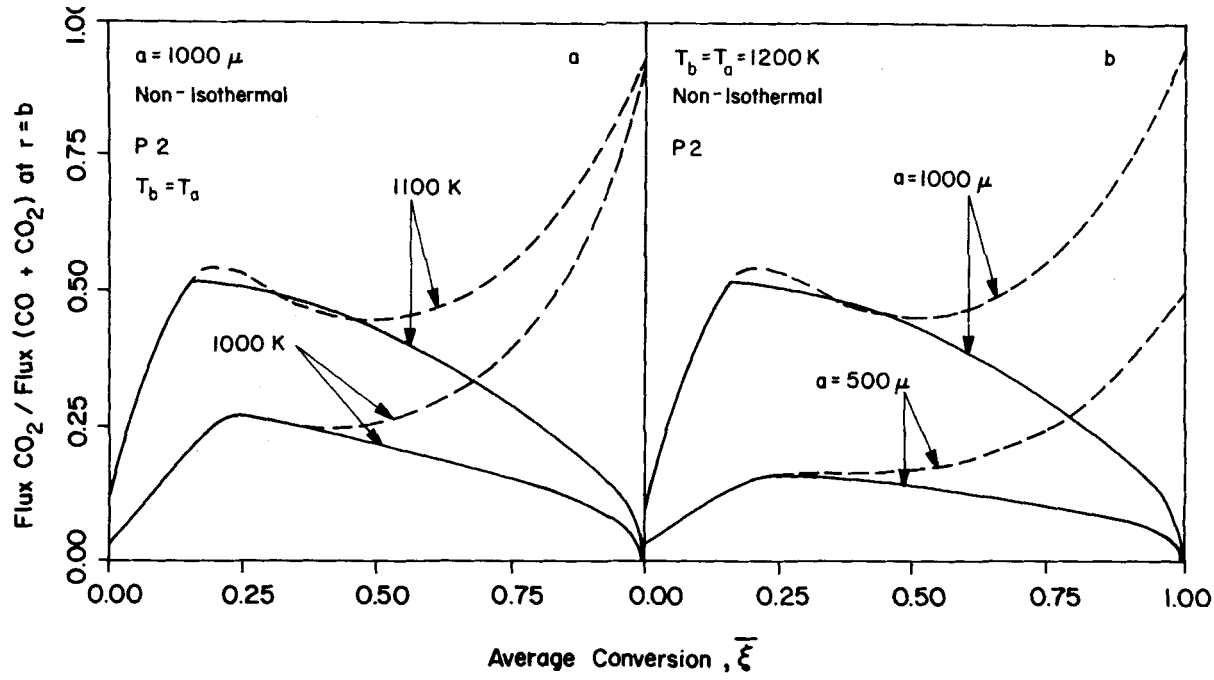

Figure 13. Variation of the relative amount of CO_2 in the products of the combustion of a single char particle with the average conversion. - - - -: nonshrinking particle.

curves and the CO_2/CO ratio starts to decrease, mainly because of the decreasing particle size.

Figures 14 and 15 present typical results for the variation of the total average conversion and of the true average conversion with time. (The true average conversion does not include the material lost in the ash.) In order to compare the predictions of the general model with the results for shrinking core behavior, we have also plotted in Figure 16 the several conversion vs. time curves given by the shrinking core model for a particle of 100 μ in radius. The shrinking core curves have been derived for pseudosteady state behavior, Fick's law for the fluxes, and CO as the only product of the combustion process. In particular, the following relation

$$\tfrac{1}{2}(1-(1-\bar{\xi})^{2/3}) - \tfrac{1}{3}(1-2\epsilon_f^2/Sh)\bar{\xi} = Kt, \qquad (7)$$

with

$$K = \frac{2\gamma\epsilon_f^2 \mathcal{D}^r M_C c^r x_{2b} \theta_d^{1/2}}{a_0^2 W_b \rho_{po}}, \qquad (8)$$

holds between $\bar{\xi}$ and t for a nonshrinking particle. If the particle shrinks disintegrating at conversion ξ^*, the shrinking core analysis gives

$$\epsilon_f^2 \xi^* (1-(1-\bar{\xi})^{2/3})/Sh = Kt \qquad (9a)$$

or

$$\epsilon_f^2 \xi^* (1-(1-\bar{\xi}_t/\xi^*)^{2/3})/Sh = Kt. \qquad (9b)$$

As expected, the time required to achieve a certain level of total average conversion decreases with decreasing critical conversion. At a given level of true average conversion, on the other hand, the radius of a shrinking particle that reacts in a shrinking core fashion is larger than the radius of another shrinking particle characterized by lower critical conversion. Consequently, the combustion rate of the former is higher, and the burning time at a certain level of true average conversion decreases with increasing critical conversion (Figure 16). This behavior is also exhibited by the results of the general model (Figure 14). When the particle falls to the unignited branch of the PSS solution, its conversion changes very slowly with time. This can be seen more clearly in Figure 15 that gives burning time results for the particles of Figure 6 and 10. Notice that negligible changes in the average conversion of the particles of Figure 15 take place in the kinetically controlled regime, although the particles spend considerably more time there.

At a given level of true average conversion, the radius of the unreacted core of a nonshrinking particle that reacts in a shrinking core fashion is larger than the radius of a shrinking particle that disintegrates at conversion $\xi^* \neq 1$. Therefore, the combustion rate of a nonshrinking particle can become higher at some value of true average conversion. For this reason, as Figure 16 shows, the burning time of a shrinking particle with $\xi^* = 0.75$ takes on higher values than the burning time of a nonshrinking particle at high true conversion values. The results of the general model (Figure 14), however, exhibit lower burning times for the nonshrinking particles at any true average conversion value. Shrinking particles reacting at 1,200 K are very close to the lower bound of the multiplicity region (Figure 1b), and hence their actual behavior deviates significantly from the shrinking core behavior. Nonetheless, as regards the behavior of the total and true average conversion with time, the general model results agree qualitatively with the predictions

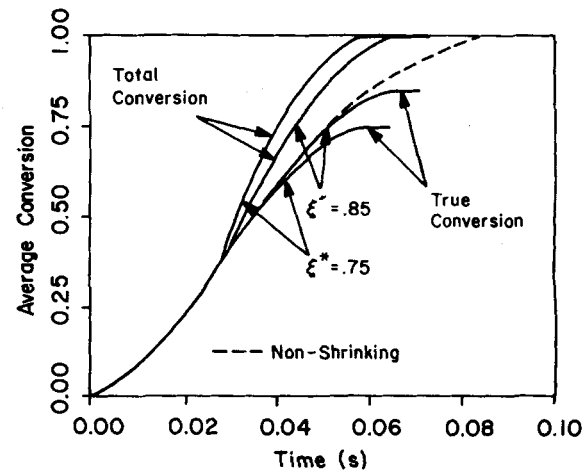

Figure 14. Variation of average conversion with time for the particles of Figure 3.

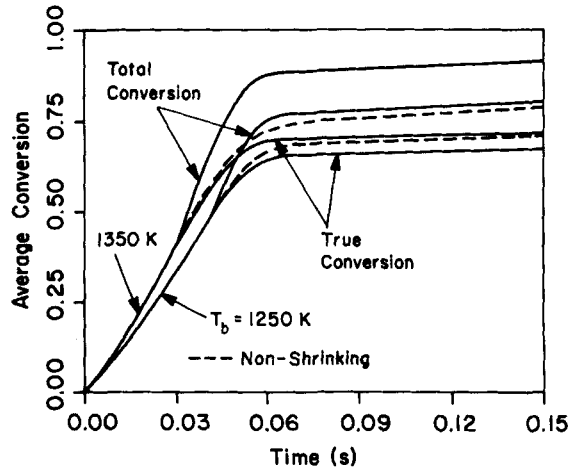

Figure 15. Variation of average conversion with time for the particles of Figure 6.

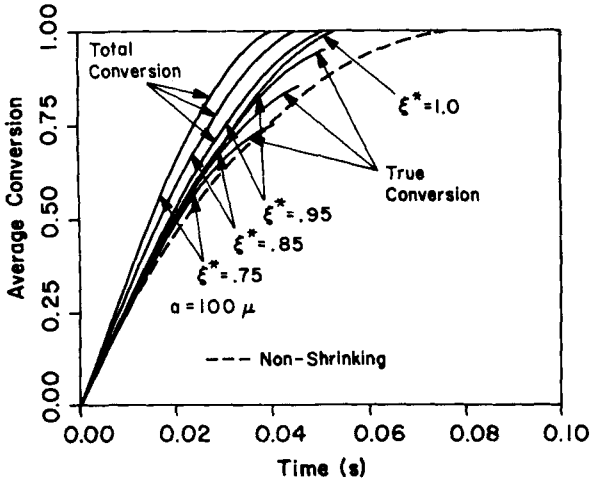

Figure 16. Variation of average conversion with time for shrinking core behavior.

of the shrinking core model (Figure 16). Extensive computations (Sotirchos, 1982) have revealed that at higher ambient temperatures the general model approaches more closely the behavior shown in Figure 16.

The rate of change of the total conversion is given by the expression

$$\frac{d\bar{\xi}}{dt} = \int_0^{\alpha} \left(\frac{\partial \xi}{\partial t}\right) d(\zeta^3) - (1 - \xi^*) \frac{d\alpha^3}{dt} \cdot \qquad (10)$$

Since the second term of Eq. 10 is discontinuous at the point where shrinkage of the particle starts, the total average conversion vs. time curves in Figures 14 and 15 go through a sharp slope change at this point. The rate of change of the true average conversion, on the other hand, is given by the first term of Eq. 10, and hence the true conversion is a smooth function of time in all cases.

ACKNOWLEDGMENT

The early phase of this work was supported by the Department of Energy. The major portion, however, was supported by the University of Houston with major grants for computer time and stipends.

NOTATION

Symbols that do not appear here are defined in Part I.

a_o = radius of the particle at $t = 0$
K = defined in Eq. 8
Sh = Sherwood number

Greek Letters

α = dimensionless radius of the particle defined in Eq. 1
β' = dimensionless distance from the center to the edge of the boundary layer defined in Eq. 1
ζ' = dimensionless distance defined in Eq. 2
ξ^* = critical conversion
$\bar{\xi}_t$ = true average conversion
τ' = dimensionless time ($\tau' = \tau$)

LITERATURE CITED

Dutta, S., C. Y. Wen, and R. T. Belt, "Reactivity of Coal and Char. 1. In Carbon Dioxide Atmosphere," *Ind. Eng. Chem., Process Des. Dev.*, **16**, p. 20 (1977).

Gavalas, G. R., "A Random Capillary Model with Application to Char Gasification at Chemically Controlled Rates," *AIChE J.*, **26**, p. 577 (1980).

Gavalas, G. R., "Analysis of Char Combustion Including the Effect of Pore Enlargement," *Comb. Sci. Technol.*, **24**, p. 197 (1981).

Groeneveld, M. J., and W. P. M. van Swaaij, "Gasification of Char Particles with CO_2 and H_2O," *Chem. Eng. Sci.*, **35**, p. 307 (1980).

Hashimoto, K., and P. L. Silveston, "Gasification: Part I. Isothermal Kinetic Control Model for a Solid with a Pore Size Distribution," *AIChE J.*, **19**, p. 259 (1973a).

Hashimoto, K., and P. L. Silveston, "Gasification: Part II. Extension to Diffusion Control," *ibid.*, **19**, p. 268 (1973b).

Ross, I. B., and J. F. Davidson, "The Combustion of Carbon Particles in a Fluidized Bed," *Trans. I. Chem. E.*, **60**, p. 108 (1982).

Sotirchos, S. V., "Diffusion and Reaction in a Char Particle and in the Surrounding Gas Phase," Ph.D. Dissertation, University of Houston, Houston (1982).

Sotirchos, S. V., and N. R. Amundson, "Diffusion and Reaction in a Char Particle and in the Surrounding Gas Phase. Two Limiting Models," *Ind. Eng. Chem. Fund.* **23**, 180 (1984).

Sotirchos, S. V., and N. R. Amundson, "Diffusion and Reaction in a Char Particle and in the Surrounding Gas Phase. A Continuous Model," *Ind. Eng. Chem. Fund.* **23**, 191 (1984).

Manuscript received January 14, 1983; revision received June 28, and accepted July 1, 1983.